BIOCHEMISTRY
including biophysical chemistry & molecular biology

Article

pubs.acs.org/biochemistry

Photoinduced Proton Release in Proteorhodopsin at Low pH: The Possibility of a Decrease in the pK_a of Asp227

Jun Tamogami,*[,†] Takashi Kikukawa,[‡] Toshifumi Nara,[†] Kazumi Shimono,[†] Makoto Demura,[‡] and Naoki Kamo[†]

[†]College of Pharmaceutical Sciences, Matsuyama University, Matsuyama, Ehime 790-8578, Japan

[‡]Faculty of Advanced Life Science, Hokkaido University, Sapporo 060-0810, Japan

Supporting Information

ABSTRACT: Proteorhodopsin (PR) is one of the microbial rhodopsins that are found in marine eubacteria and likely functions as an outward light-driven proton pump. Previously, we [Tamogami, J., et al. (2009) *Photochem. Photobiol. 85*, 578−589] reported the occurrence of a photoinduced proton transfer in PR between pH 5 and 10 using a transparent ITO (indium−tin oxide) or SnO_2 electrode that works as a time-resolving pH electrode. In the study presented here, the proton transfer at low pH (<4) was investigated. Under these conditions, Asp97, the primary counterion to the protonated Schiff base, is protonated. We observed a first proton release that was followed by an uptake; during this process, however, the M intermediate did not form. Through the use of experiments with several PR mutants, we found that Asp227 played an essential role in proton release. This residue corresponds to the Asp212 residue of bacteriorhodopsin, the so-called secondary Schiff base counterion. We estimated the pK_a of this residue in both the dark and the proton-releasing photoproduct to be ∼3.0 and ∼2.3, respectively. The pK_a value of Asp227 in the dark was also estimated spectroscopically and was approximately equal to that determined with the ITO experiments, which may imply the possibility of the release of a proton from Asp227. In the absence of Cl^-, we observed the proton release in D227N and found that Asp97, the primary counterion, played a key role. It is inferred that the negative charge is required to stabilize the photoproducts through the deprotonation of Asp227 (first choice), the binding of Cl^- (second choice), or the deprotonation of Asp97. The photoinduced proton release (possibly by the decrease in the pK_a of the secondary counterion) in acidic media was also observed in other microbial rhodopsins with the exception of the *Anabaena* sensory rhodopsin, which lacks the dissociable residue at the position of Asp212 of BR or Asp227 of PR and halorhodopsin. The implication of this pK_a decrease is discussed.

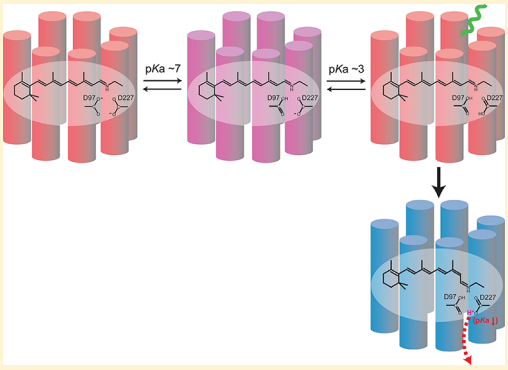

Microbial rhodopsins are photoactive membrane proteins that contain retinal as a chromophore. They were originally found in Archaea as bacteriorhodopsin (BR),[1,2] halorhodopsin (HR),[3−5] sensory rhodopsin I (SRI),[6−8] and sensory rhodopsin II (SRII).[9−12] The recent advance in genome technology has allowed the detection of the genes that encode microbial rhodopsins in many microorganisms. These proteins have now also been discovered in eubacteria[13−15] and lower eukaryotes, such as fungi[16,17] and algae.[18−21] Thus, it was revealed that microbial rhodopsins are broadly distributed in the biosphere now. One of the typical examples is PR, which is found in marine eubacteria.[22] To date, more than 800 variants of PR have been found in the ocean.[23] It has been believed that PR works as a light-driven proton pump like BR.[13] Since the discovery of PR, many studies of the photochemical properties of PR have been conducted.[24−32] Although there are a few differences, the photocycle scheme of PR is similar to that of BR.[24−27] The residues that are important for the function of PR have also been identified. For instance, it has been revealed that Asp97 and Glu108 act as the acceptor of a proton from the protonated Schiff base (PSB, or counterion to the positively charged PSB) and the donor of a proton to the deprotonated Schiff base (SB), respectively.[24,25,28] In BR, Asp85, a proton acceptor, and Asp212 are located near and arranged symmetrically around the PSB such that these two residues form a so-called pentagon cluster with three water molecules. Thus, both Asp85 and Asp212 may be members of the proton acceptor cluster. In spite of this structure and the emphasized importance of Asp212, the primary proton acceptor is Asp85. Similarly, Asp227 of PR, which corresponds to Asp212 of BR, is reported to be an important residue.[30,31] In addition, this residue has been found to control the photoisomerization,[32] and its neutralization affects the formation of a long-lived photoproduct.[32,33] In this paper, we refer to Asp227 (Asp212 of BR) as a secondary proton acceptor or counterion of the PSB.

The measurement of the transfer of a proton between the protein and the external medium is important for the

Received: July 14, 2012
Revised: October 23, 2012
Published: October 24, 2012

elucidation of the photochemistry of microbial rhodopsins. The standard method for the measurements of proton transfer is to measure the change in the pH of the medium through the using of pH indicator dyes.[34] However, this method has a disadvantage in that it can be used only if it can be applied to the medium whose pH is close to the pK_a of the dye. We and Koyama et al. therefore devised an electrochemical cell using a transparent ITO (indium−tin oxide) or SnO_2 electrode that can monitor the time-resolving pH change of the medium at any pH.[35−37] Previously, using a SnO_2 electrochemical cell, we observed the first proton uptake and subsequent release of the PR in the pH range from 4 to 9.5.[37] The dependence of pH on the magnitude of the proton uptake agreed with the degree of deprotonated Asp97, the primary counterion in the dark. However, there were small differences found in the pH range of 4−5 (see Discussion).[37] In this paper, using the ITO electrode method, we examined the photoinduced proton transfer in the PR at pH <4. In acidic media, in which both the primary and secondary counterions are protonated, we first observed the release of a proton, which was then followed by the uptake of a proton. From the pH profile, we estimated pK_a values of a key residue in unphotolyzed and photolyzed states. Using various mutant experiments, we found that a key residue was Asp227, the secondary counterion. The pK_a of this residue in the unphotolyzed state was spectroscopically determined, which is approximately equal to that determined from ITO. Assuming that the proton is released from Asp227, the implication of the decrease in the pK_a of Asp227 is discussed. In addition, we observed the release of a proton from D227N mutant in the absence of Cl^- and found that the protonated primary counterion (proton acceptor), Asp97, was involved.

MATERIALS AND METHODS

Construction of Expression Plasmids for PR Mutants. The expression plasmids of the PR mutants (R94K, R94Q, D97E, D97N, D227E, D227N, and D97N/D227N) were prepared by polymerase chain reaction (PCR) using the QuikChange site-directed mutagenesis kit (Stratagene). The designed primers were as follows: R94K, 5′-CCAACTGTATTTAAATACATTGATTGG-3′ and 5′-CCAATCAATGTAATTTAAATACAGTTGG-3′; R94Q, 5′-CCAACTGTATTTCAATACATTGATTG-3′ and 5′-CAATCAATGTAATTGAAATACAGTTGG-3′; D97E, 5′-TTTAGATACATTGAGTGGTTACTA-3′ and 5′-TAGTAACCACTCAATGTATCTAAA-3′; D97N, 5′-TTTAGATACATTAATTGGTTACTA-3′ and 5′-TAGTAACCAATTAATGTATCTAAA-3′; D227E, 5′-AACCTTGCTGAGTTTGTTAACAAG-3′ and 5′-CTTGTTAACAAACTCAGCAAGGTT-3′; D227N, 5′-CTATAACCTTGCTAACTTTGTTAAC-3′ and 5′-GTTAACAAAGTTAGCAAGGTTATAG-3′. The underlined bases indicate those that encode the mutated amino acids. The sequences of the PCR products were confirmed using an automated sequencer (377 DNA sequencer, Applied Biosystems, Foster City, CA).

Preparation of Proteins. The expression plasmids of PR (pBAD/PR, EBAC31A08, GenBank entry AF279106)[13] and ASR (*Anabaena* sensory rhodopsin) from *Anabaena* sp. PCC7120 (pMS107/ASR)[14] were provided by O. Béjà and K.-H. Jung, respectively. The expression plasmids of HsSRII (SRII from *Halobacterium salinarum*),[38] NpSRII (SRII from *Natronomonas pharaonis*),[39] and HmSRIII (SRIII from *Haloarcula marismortui*)[40] were constructed previously. *Escherichia coli* UT5600 cells were used for the expression of PR and its mutants, whereas *E. coli* BL21-CodonPlus (DE3)-RP cells (Stratagene, La Jolla, CA) were used for the expression of ASR, HsSRII, NpSRII, and HmSRIII. The expression and preparation of the proteins were performed as described previously.[37−40] The purified proteins were reconstituted into L-α-phosphatidylcholine (PC) from egg yolk (Avanti, Alabaster, AL) at a protein:PC molar ratio of 1:50. The procedure of the PC reconstitution of proteins was the same as that described previously.[37] The reconstituted proteins were washed thoroughly with distilled water by centrifugation and used for experiments after they had been suspended in the proper medium prior to use.

BR was prepared from *H. salinarum* strain S9 through the established standard method.[41] The XR proteins from *Salinibacter ruber* were provided by J. K. Lanyi and S. P. Balashov. These two proteins were suspended in distilled water and used for the experiments.

Measurement of Photoinduced Proton Uptake and Release by an ITO (indium−tin oxide) Electrode. The apparatus and procedure were essentially the same as those described previously.[37] For the adsorption of proteins onto the ITO surface, the protein concentration of the PC-reconstituted samples (PR, ASR, HsSRII, NpSRII, and HmSRIII) and proteins from native membranes (BR and XR) suspended in distilled water was ∼2−6 μM. The amount of proteins attached to the electrode surface was estimated to be $\sim 1.5-4.6 \times 10^{14}$ molecules/cm^2. The electric signals were measured with an AC amplifier (MEG-1200, Nihon Koden, Tokyo, Japan) equipped with a 0.08 Hz low-cutoff electric filter. The electric signals were stored in a microcomputer and accumulated five times to obtain the averaged signal. The light source was a 300 W xenon lamp with a combination of a cold mirror, an IR filter (HA50, Toshiba, Tokyo, Japan), and a cutoff optical filter (Y44, Toshiba) to excite the protein. The duration of the light was modulated to 2 ms by using a mechanical shutter. The measurements were performed in solutions containing an electrolyte (NaCl or Na_2SO_4) and a buffer (glycine or citrate) that was adjusted to the desired pH with HCl (or H_2SO_4) and NaOH. Details of the consideration of the buffering solution are given in the Supporting Information, in which the reason for the use of 1 mM glycine or citrate is given. The experiments were performed at room temperature (20−25 °C).

UV−Visible Spectroscopy. A spectrophotometer (U-3310, Hitachi, Tokyo, Japan) was employed for measurements of the absorbance spectra. The temperature was maintained at 20 °C with a thermostat (Uni Ace UA-1100, Eyela-Digital, Tokyo, Japan). The PC-reconstituted PR proteins (at ∼10 μM) were encapsulated into a 15% polyacrylamide gel to prevent their aggregation during the measurements. To remove the effect of the scattering from the spectra and to estimate λ_{max}, the observed absorption spectra were fit to the following skewed Gaussian equation (eq 1).

$$\mathrm{Abs}(\lambda) = A + \frac{B}{\lambda^C} + \sum_{i=1}^{k} \varepsilon_{i,\max} \times \exp\left(-\frac{\ln 2}{(\ln \rho_i)^2} \left\{ \ln\left[\frac{(1/\lambda - 1/\lambda_{i,\max})(\rho_i^2 - 1)}{\Delta\nu_i \times \rho_i} + 1 \right] \right\}^2 \right) \quad (1)$$

where Abs(λ) is the absorbance, λ_{max} is the absorbance maximum, ε_{max} is the maximal extinction, ρ is the parameter of skewness, and $\Delta\nu$ is the half-bandwidth. The first term (A) is

dx.doi.org/10.1021/bi300940p | Biochemistry 2012, 51, 9290−9301

an offset, and the second term expresses the background scattering line.[42] The obtained spectra could be described sufficiently by the linear combination of three (and five for spectra of D227E at a pH above ~6) skewed Gaussian functions.

Flash-Photolysis Spectroscopy. The apparatus and procedure for flash-photolysis were essentially the same as those reported previously.[43] The transient absorption changes induced by a laser pulse (Nd:YAG 532 nm, 7 ns, 5 mJ/pulse) were acquired by using a computer at intervals of 0.5 μs between −40.1 and 222 ms. The data before the laser pulse were used as a baseline. The temperature was controlled at 20 °C using a thermostat (Eyela-Digital Uni Ace UA-110). The suspension of the PC-reconstituted samples was used for the measurements. The protein concentration was ~10 μM. The global fitting was performed for the obtained data according to the sequential irreversible model in which the existence of a reversible or branched reaction is not assumed, although molecules were a mixture of protonated and deprotonated Asp227 at pH 3.5. The method of global fitting was the same as that described previously.[44]

RESULTS

First Release of a Proton from PR in Acidic Media. The pK_a of the primary counterion, Asp97, of PR in the unphotolyzed state was estimated to be 7−8.[24,25,27,29,32] At neutral or alkaline pH higher than this pK_a, the proton moves from the PSB to Asp97 by illumination such that the M intermediate (abbreviated M hereafter) is formed. The proton uptake occurs during the decay of M (i.e., the formation of the following intermediate or N intermediate, abbreviated N), and release occurs during the decay of N.[24] However, in acidic media, Asp97 is protonated in the unphotolyzed state, which means that the transfer of the proton from the PSB to Asp97 should not occur. Actually, the formation of M with a deprotonated Schiff base was not observed.[24,25,27,28] In spite of this finding, we observed the first proton release and subsequent uptake of a proton at a pH below ~4. Figure 1 shows the photoinduced ITO signals, which indicate the first proton release (upward shift) followed by the uptake (downward shift). To reconfirm that the deflection comes from the change in the pH of the medium, we verified the dependence of the buffer (glycine) concentrations in the ITO cell. The results in Figure 1 show that the magnitude decreases with an increase in the buffer concentration and these changes have the same shape. Thus, we conclude that the results shown in Figure 1 reveal that the photoinduced early proton release can occur without the deprotonation of the PSB at pH 3.

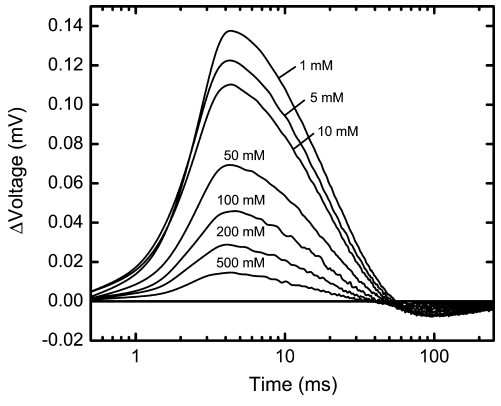

Figure 1. Proton transfer signal in PR at low pH at varying buffer concentrations. The respective traces show the photoinduced proton transfer signals in the presence of 1, 5, 10, 50, 100, 200, and 500 mM glycine from top to bottom, respectively. The magnitude decreases as the buffer concentration increases. The medium contained 0.4 M NaCl at pH 3.0. The concentration of the PC-reconstituted proteins adsorbed onto the ITO electrode surface was ~6 μM.

pH Dependence of the Initial Proton Release at Low pH. We examined the photoinduced proton transfer over a pH range of 1.75−4.0 using a medium containing 0.4 M NaCl and 1 mM glycine. With respect to the selection of the buffer solution, see the Supporting Information. As the pH increased from 1.75 to 2.75, the magnitude of the signal increased; however, an additional increase in pH resulted in a decrease in the magnitude of the signal. The solid and broken lines in Figure 2a represent the traces measured between pH 1.75 and 2.75 and between pH 2.75 and 4.0, respectively. As shown in the figure, the shapes of solid lines are almost very similar to one another, which implies that the kinetics may be constant in this pH region. However, the rate constants of proton release at pH >2.75 decrease with an increase in pH. At pH 3.5−4.0, the

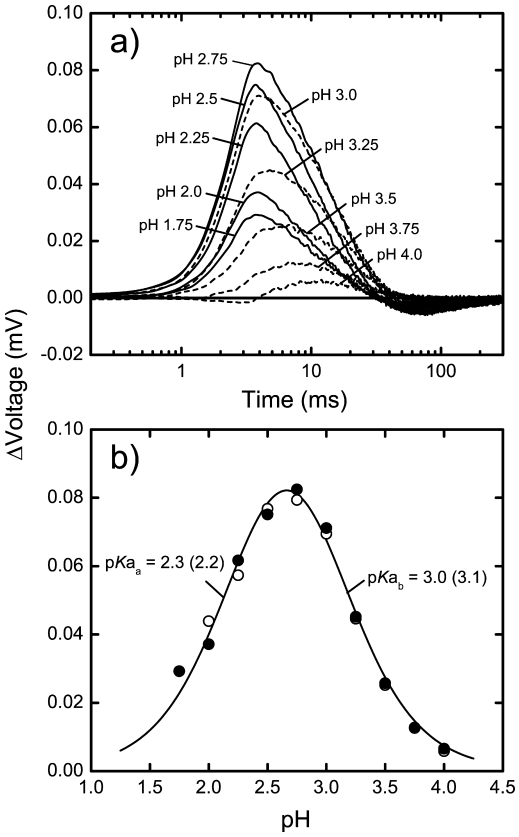

Figure 2. pH dependence of the photoinduced proton transfer signal in PR under low-pH conditions. (a) Time-dependent and photoinduced proton transfer signals at varying pH values. The media contained 0.4 M NaCl and 1 mM glycine. The pH of the media was adjusted to the desired value through the addition of HCl or NaOH. The concentration of the PC-reconstituted proteins absorbed onto the ITO electrode surface was ~3 μM. (b) Plot of the peak value of the photoinduced signals as a function of medium pH. The filled circles are the data obtained using glycine buffer, which is shown in panel a, whereas the empty circles represent data obtained using the medium containing 1 mM citrate.

dx.doi.org/10.1021/bi300940p | Biochemistry 2012, 51, 9290−9301

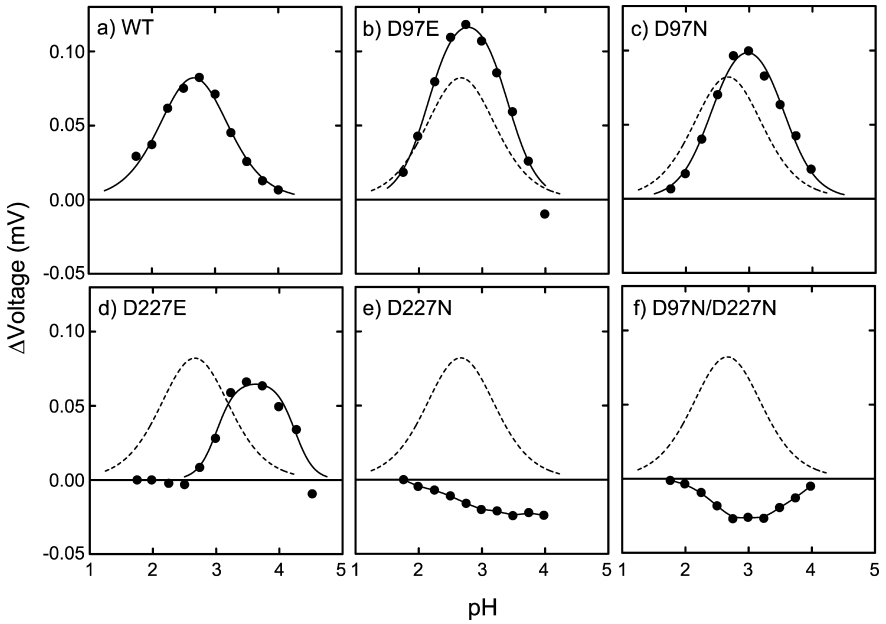

Figure 3. Comparison of the pH profiles of the photoinduced proton transfer signals in the wild type and several PR mutants: (a) WT, (b) D97E, (c) D97N, (d) D227E, (e) D227N, and (f) D97N/D227N. The experimental conditions were the same as those used to obtain the data in Figure 2a. The broken lines in panels b–f represent the data obtained with the wild type.

delay was clearly observed. We performed similar experiments using 1 mM citrate instead of glycine, and no essential differences were obtained. The reason for the coincidence using two buffer solutions is given in the Supporting Information. In Figure 2b, the peak values from Figure 2a are plotted versus pH. The filled circles indicate the values obtained using glycine buffer, whereas the empty circles are those values obtained with the citrate buffer. As shown in this figure, a bell-shaped pH profile is obtained. This bell-shaped profile can be explained assuming the existence of an X-H residue from which a proton is released. Therefore, this X-H residue is protonated in the dark. The decrease in the amplitudes with an increase in pH (the right half of Figure 2b) can be explained by the dissociation of the X-H residue in the dark. To obtain the photoinduced proton release, the X-H residue should dissociate such that its pK_a at the proton-releasing photoproducts is lower than the pH in the medium. Consequently, the proton release should become more difficult as the pH in the medium decreases, which explains the left half of the bell curve in Figure 2b. On the basis of this hypothesis, the bell-shaped curve was fit with the following equation:

$$\Delta\text{voltage} = A\left[\frac{1}{1 + 10^{n_a(pK_{aa}-pH)}}\right]\left[\frac{1}{1 + 10^{n_b(pH-pK_{ab})}}\right] \quad (2)$$

where pK_{aa} and pK_{ab} are those pK_a values of the X-H residue at the proton-releasing state and in the dark, respectively, A is a constant scaling the amplitude, and n_a and n_b are Hill coefficients. The estimated pK_{aa} values were 2.3 and 2.2 for the glycine and citrate buffers, respectively, and the pK_{ab} values were 3.0 and 3.1 for the glycine and citrate buffers, respectively. Thus, we conclude that upon illumination, the pK_a of the X-H residue decreases from ∼3 to 2.

Identification of the X-H Residue. However, although we hypothesized the existence of an X-H residue, its identity was unknown. The PSB can be excluded as a candidate, because the M intermediate with the deprotonated SB was not formed (pH ≪ pK_a of the counterion). As described previously, the pK_a of the X-H residue in the dark was estimated to be ∼3, which suggests that an acidic amino acid residue may be a candidate. Therefore, various Asp and Glu mutants such as E50Q, D52N, E85Q, D88N, E108Q, E142Q, E165Q, E170Q, and D212N were examined; however, the response of these mutants was the same as that of the wild type (data not shown). Nevertheless, different behaviors were observed with several PR mutants of the primary (Asp97) and secondary (Asp227) counterions to the PSB. Figure 3 shows the plots of the peak values as a function of the pH for these mutants. The data of D97E and D97N essentially show a pH profile that is the same as that of the wild type, but the peak pH shifted slightly toward alkaline (∼0.5 unit) (see Table 1). Figure 3d shows the large pK_a

Table 1. pK_a Values of Asp227 in the Wild Type and Various PR Mutants Determined with the ITO Experiments

	H^+-releasing (pK_{aa})	dark (pK_{ab})
WT[a]	2.3	3.0
D97E[a]	2.1	3.4
D97N[a]	2.4	3.5
D227E[a]	3.0	4.2
D227N	–	–
D97N/D227N	–	–
R94Q[b]		
Cl^- (−)	2.7	3.8
Cl^- (+)	2.4	3.8
R94K[b]		
Cl^- (−)	3.1	3.7
Cl^- (+)	>∼3.1[c]	<∼3.7[c]

[a]The pK_a values of WT, D97E, D97N, and D227E were estimated by fitting the data obtained at 0.4 M NaCl (Figure 3). [b]In the case of R94Q and R94K, Cl^- (−) represents the values obtained using 0.333 M Na_2SO_4 whereas Cl^- (+) represents the values obtained using 1 M NaCl. [c]These values have some ambiguity because of the complex pH behavior (Figure 6b).

dx.doi.org/10.1021/bi300940p | *Biochemistry* 2012, 51, 9290–9301

increase of the X-H residue in both the dark and the proton-releasing photoproduct when Asp227 is replaced with Glu. Of particular interest, the first proton release phase disappeared in the D227N and D97N/D227N mutants, and the proton uptake occurred first. For these mutants, we observed the first proton uptake, and its origin is not clear at present. As described in the Supporting Information, the assumption of the existence of residue Y is indispensable for the analysis of the behavior of the spectrum of D227N whose pK_a was estimated to be 3.2−4.5 depending on the Cl^- concentration. There is a possibility that illumination induces the conformational change to induce the proton transfer via this residue only in the D227N mutant. Further study is necessary. In spite of this, these results suggest that the hypothetical X-H residue is Asp227. Although the possibility of the release of the proton from the protonated water cluster cannot be excluded completely, it is certain that Asp227 plays a key role.

Effect of Cl^- on the Proton Transfer of the Wild Type at Low pH. We then measured the proton transfer of the wild type at various Cl^- concentrations. As shown in Figure 4a, the pH profiles shifted to a lower pH (by ~0.3) with an increase in the chloride concentration in the medium. The pK_a values for both the unphotolyzed and photolyzed states that were estimated using eq 2 decreased as the Cl^- concentration increased (refer to the legend of Figure 4). Figure 4b shows the differences in the pK_a values of the photolyzed (●) and unphotolyzed states (○) compared to those in Cl^--free medium. A Cl^- concentration of 0.4 M results in pK_a changes that are half of the maximal changes measured in both photolyzed and unphotolyzed states. Figure 4c shows the time course of the proton transfer signals at varying Cl^- concentrations. The rates of the uptake phase decrease with an increase in the Cl^- concentration. These Cl^--dependent proton uptake rates, combined with the Cl^--dependent pK_a change of Asp227 (Figure 4b), may be interpreted in two ways: (1) Cl^- binding near Asp227 and Arg94 and (2) the effect of an electric double layer on the protein surface. The latter hypothesis is ruled out because the experiments were performed under constant-ionic strength conditions. Therefore, this Cl^- dependence is ascribed to Cl^- binding maybe in the vicinity of Asp227 and positively charged Arg94. The negative charge of Cl^- may retard proton release, which results in a decrease in the peak values observed in Figure 4c. However, the reason why the increase in the negative charge due to the binding of Cl^- does decrease the pK_a of Asp227 is problematic because the increase in negative charge near the residue should hinder the positively charged proton release, which would increase the pK_a. However, it is possible that Cl^- binding might stabilize the dissociated state of Asp227 because of perhaps changes in the hydrogen bonding or water structure.

The Absence of Cl^- Drastically Changes the Proton Transfer of D227N at Low pH. As described in the legend of Figure 3e, we did not observe the first proton release from D227N in low-pH solutions, which gave a probability that the proton release originates in Asp227 at low pH, although the origin and the mechanism of the proton uptake in Figure 3e are not known (one of possibilities is described above). Note that these results were obtained in the presence of 0.4 M Cl^-. We therefore examined the effect of Cl^- on the proton transfer of the D227N mutant. Interestingly, we found the unexpected first release of a proton from D227N in the absence of Cl^- (see Figure 5a) even though the putative residue responsible for the first proton release (Asp227) was neutralized. Therefore, we

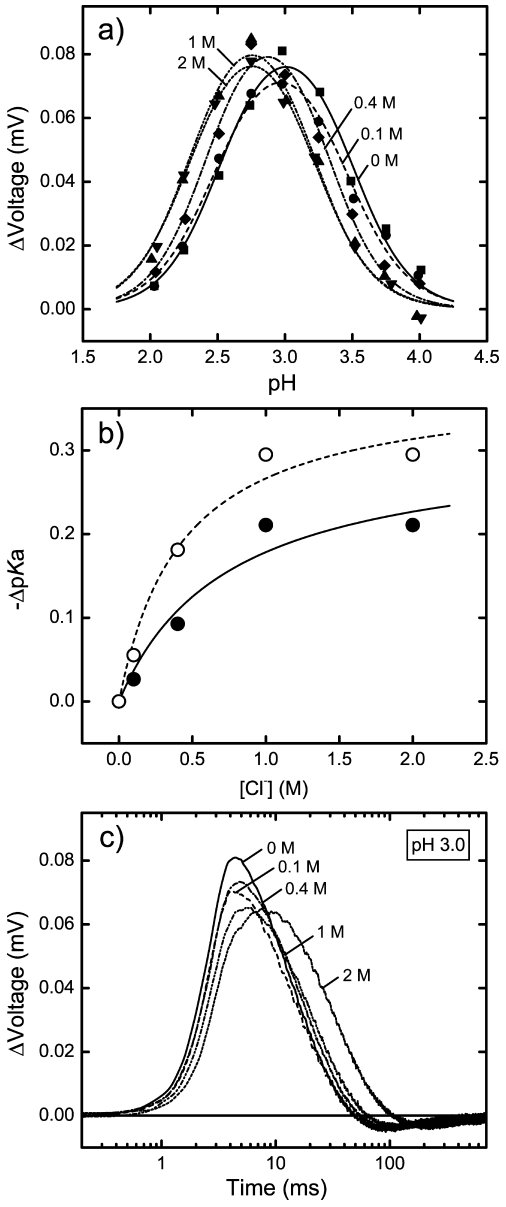

Figure 4. Photoinduced proton transfer in the wild type at varying chloride concentrations. (a) pH profiles of the proton releasing signals in the presence of 0 (■), 0.1 (●), 0.4 (◆), 1 (▲), and 2 M chloride (▼). The data obtained at each NaCl concentration were fit by eq 2 to estimate the pK_{aa} and pK_{ab} values. The estimated pK_{aa} values for 0, 0.1, 0.4, 1, and 2 M chloride were 2.52, 2.49, 2.43, 2.31, and 2.31, respectively, whereas the pK_{ab} values were 3.50, 3.44, 3.32, 3.20, and 3.20, respectively. The medium contained 1 mM glycine and was adjusted to the desired pH through the addition of H_2SO_4 or NaOH. The total ionic strength in the solution was kept constant through the addition of the appropriate concentration of Na_2SO_4. The concentration of the PC-reconstituted proteins adsorbed onto the electrode surface was ~3 μM. (b) Plot of the difference in the pK_a (ΔpK_a) values as a function of Cl^- concentration. The reference values are those obtained in the absence of Cl^-. The filled and empty circles are plots of ΔpK_{aa} (in the photolyzed state) and ΔpK_{ab} (in the unphotolyzed state), respectively. These changes are ascribed to the binding of Cl^-. The K_d value of Cl^- is estimated to be ~0.4 M. (c) Proton transfer as a function of time at varying Cl^- concentrations (at pH 3.0). The traces shown from left to right were obtained in the presence of 0, 0.1, 0.4, 1, and 2 M Cl^-, respectively.

dx.doi.org/10.1021/bi300940p | *Biochemistry* 2012, 51, 9290−9301

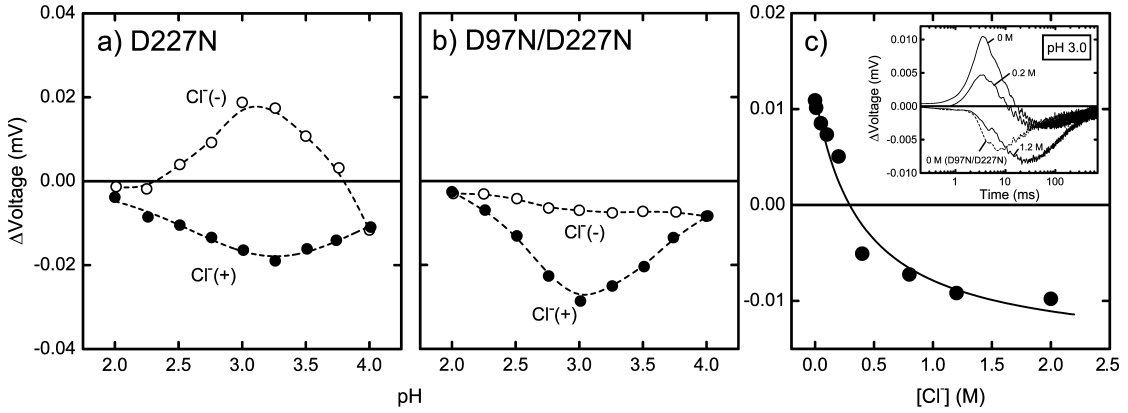

Figure 5. Effect of chloride on the photoinduced proton transfer in the D227N mutants. (a) pH profile of photoinduced proton transfer signals in D227N. The medium contains 1 mM glycine and 1 M NaCl (●) or 0.333 M Na_2SO_4 (○). The preparation of the protein film on the electrode surface was the same as in Figures 2–4. (b) Plot for D97N/D227N. The symbols are the same as in panel a. (c) Cl^- dependence of the photoinduced proton transfer signals in D227N. The peak values of the photoinduced proton release or uptake signals that appear initially (exemplary traces are shown in the inset) were plotted against the Cl^- concentration. The measurements were performed in a solution containing 1 mM glycine and various concentrations of NaCl (0–2 M) at pH 3.0. The total ionic strength of the solution was kept constant through the addition of the appropriate concentration of Na_2SO_4. This Cl^--dependent change may be ascribed to the binding of Cl^- (see the text), which was estimated to have a K_d of ~0.4 M.

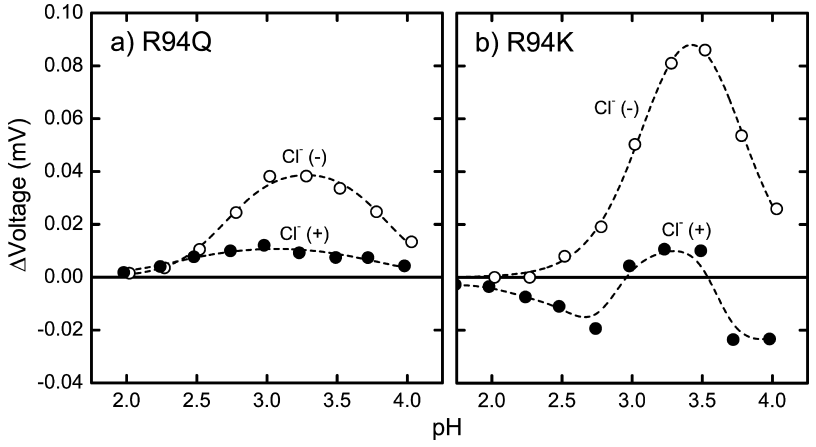

Figure 6. pH profile of the photoinduced proton transfer signals at low pH with Arg94 mutations in PR: (a) R94Q and (b) R94K. The empty and filled circles indicate the data obtained in the absence (ionic strength adjusted to 1 M with Na_2SO_4) and presence of Cl^- (1 M NaCl), respectively. The experimental conditions were the same as those used to obtain the data in Figure 5a.

investigated the identity of the residue that is responsible for the proton release in D227N and found that the key residue is Asp97 in acidic media. We performed the experiment using the D97N/D227N double mutant and did not observe the first proton release in the presence or absence of Cl^-, although the unexplained proton uptake occurred (panel Figure 5b and see above). Therefore, via the first proton release in D227N in the absence of Cl^- (Figure 5a), we deduced that the primary counterion of the PSB, Asp97, plays an essential role and that there is a possibility that Asp97 itself may be an origin of proton release. Figure 5c shows the amplitudes of the peak values of the photoinduced signals of the D227N mutant at pH 3.0 at varying Cl^- concentrations; as shown, these values change from positive (proton release) to negative (uptake) as the concentration of Cl^- increases. This finding may be interpreted as follows: Cl^- binds to the vicinity of neutral Asn (at position 227), potentially to the positively charged Arg94, and the K_d of this binding is ~0.4 M (see Figure 5c), which is almost equal to that shown in Figure 4b. In summary, in the D227N mutant, the photoinduced proton release occurs first in the absence of Cl^-, and Asp97 is involved in the release. In the presence of Cl^-, the release is not observed, which is due to the negative charge created by the Cl^- binding (K_d ~ 0.4 M) at the position of neutralized Asp227. The pK_a values of the residue controlling the proton release in D227N in the unphotolyzed and photolyzed states were not determined because the presence of the proton uptake phase prevented an exact estimation. The mechanism and/or origin of this uptake is not known at present. One of the possibilities is described above.

Role of Arg94 in the First Proton Release at Low pH. As found in BR or other microbial rhodopsins, an important arginine residue is located in the vicinity of the counterions (primary and secondary) and interacts with them through water molecules. Therefore, the influence of a mutation at this position (Arg94 in PR) on the first proton release at low pH was also investigated. Panels a and b of Figure 6 show the pH profiles of the photoinduced proton transfer signals obtained from R94Q and R94K, respectively. In the R94Q mutant, the first proton release occurred regardless of the presence of Cl^-, although the magnitudes are different. The fact that the first

dx.doi.org/10.1021/bi300940p | *Biochemistry* 2012, 51, 9290–9301

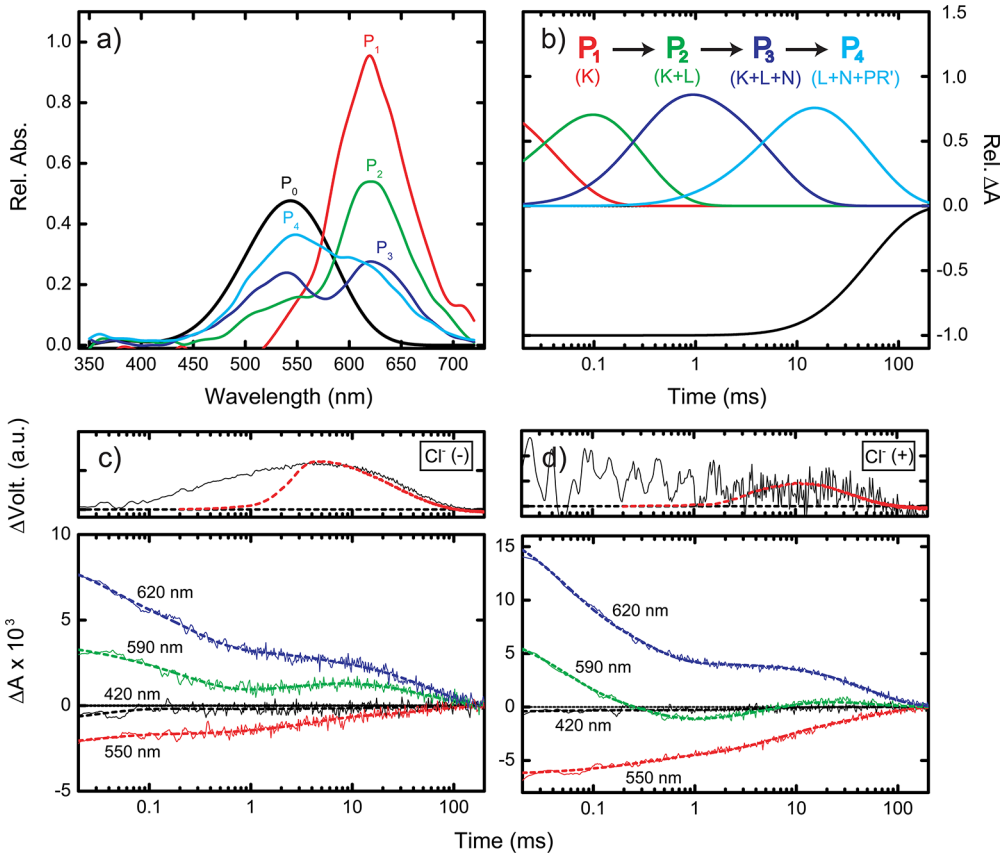

Figure 7. Flash-induced absorbance changes of PR under low-pH conditions. (a) Absorbance spectra of each state in a medium containing 0.4 M NaCl and 1 mM glycine at pH 3.5. The PC-reconstituted proteins at a concentration of ~10 μM were used for the measurements. P_0 shows the spectrum of the unphotolyzed state from which the scattering was removed, whereas P_1–P_4 are those of the kinetically defined states calculated by global fitting. The absorbances of the respective spectra were normalized at the amplitude of the absorbance of P_1 at its λ_{max}. The spectra of P_0–P_4 are colored black, red, green, blue, and cyan, respectively. (b) Time-dependent absorbance traces of each state (P_1–P_4). The colors of the traces are the same as those used in panel a. (c) Comparison of the photoinduced proton transfer signal and absorbance change signal in the absence of Cl^- (in the presence of 0.133 M Na_2SO_4) at pH 3.5. The top panel shows the photoinduced proton transfer signals obtained with the ITO experiments. The black solid line and red broken line are the signals obtained using irradiation of the laser pulse and a 2 ms flash light, respectively. The bottom panel indicates the photoinduced absorbance change signals measured at four wavelengths. The noisy (solid) and smooth (broken) lines indicate the observed data and the fitting curves, respectively. (d) Comparison of the photoinduced proton transfer signal and absorbance change signal in the presence of 0.4 M NaCl at pH 3.5. The data plotted are similar to those shown in panel c.

proton release was observed in R94Q implies that the first proton release does not originate from Arg94. The pK_a values of the proton transfer were estimated using eq 2 and are listed in Table 1. The pK_a values of the proton releasing state (from possibly Asp227) are smaller than those of the unphotolyzed state because this state is the same as the wild type, and the estimated values are slightly different from those of the wild type. This is consistent with the notion that weak coupling exists between the conserved arginine and the chromophore and its counterion.[29] As in the wild type (Figure 4c), the deflections of the ITO electrode potential in the absence of Cl^- are larger than those in the presence of Cl^-, and the difference between these deflections is much greater than the difference observed with the wild type. Although the reason is not clear at present, the loss of the positive charge through the mutation of Arg94 might be a cause. In the R94K mutant (Figure 6b), on the other hand, proton release occurred in the absence of Cl^- and the behavior of the magnitude as a function of pH is simple, whereas the behavior in the presence of Cl^- is complicated, for reasons that are not yet clear. The binding of Cl^- near Lys at position 94 might cause the complicated pH profile.

Comparison of the Time Course of Proton Transfer with That of Flash-Photolysis Data. Flash-photolysis experiments were also performed to investigate the point at which the photoinduced H^+ release and/or uptake of PR occurs at low pH. A global fitting was performed for data obtained with PR in the presence of 0.4 M Cl^- at pH 3.5. The data were fit sufficiently with the equation using a sum of four exponential terms. Figure 7a shows the obtained spectra of kinetically defined states (from P_1 to P_4). After illumination, the largely red-shifted state (λ_{max} ~ 620 nm) was formed, which is most likely the K intermediate. The following state, P_2, contains the component from P_1 and other components having absorption around 500–550 nm. The peak of this absorption was close to that of the unphotolyzed PR (P_0), although it was slightly blue-shifted. Generally, this blue-shifted component may be considered to be the L intermediate. In the next state (P_3), the magnitude of the absorption band of L increases, whereas the magnitude of the red-shifted absorption band decreased. Furthermore, the bandwidth of the red-shifted absorption band became somewhat broad, which indicates the contaminant of another red-shifted intermediate (most likely the N intermediate). In the final state (P_4), the increase in the absorbance

dx.doi.org/10.1021/bi300940p | *Biochemistry* 2012, 51, 9290–9301

at a wavelength close to P_0 (λ_{max} ~ 550 nm) was observed, which may indicate the formation of the PR′ intermediate. Thus, the observed photocycle scheme containing the K, L, N, and PR′ intermediates (and not the M intermediate) is in agreement with the previous report.[25,27] The respective time constants of the P_1−P_4 states were estimated to be 0.05, 0.3, 6.7, and 56 ms, respectively. Panels c and d of Figure 7 show the comparison of the ITO signals (top panels) and flash-photolysis signals (bottom panels) in the absence and presence of Cl^-, respectively. Here, the ITO signals photoinduced by a 2 ms flash light excitation (see the red broken lines in the top panels of Figure 7c,d) contain inaccuracy before ~10 ms.[37] Therefore, we used a laser pulse as the light source instead of a xenon lamp. In the absence of Cl^-, the proton release occurred in the range of several hundred microseconds, whereas it occurred in the range of several milliseconds in the presence of Cl^- (see the black solid lines in the top panels of Figure 7c,d). In addition, proton uptake occurred in the range of several hundred milliseconds in the absence and presence of Cl^-. The exact identification of the intermediates associated with H^+ release and/or uptake was difficult from these results. However, it can at least be inferred that the H^+ release occurs after the decay of the K intermediate (and most likely the decay of the L intermediate as well) and the H^+ uptake occurs during the latter half of its photocycle (most likely the decay of the N or PR′ intermediate).

Shift in the Absorbance Spectrum of PR at Low pH: Determination of the pK_a of Asp227 at Unphotolyzed PR. It has been known that the dissociation and association of the two counterions lead to the change in the absorbance spectra. For example, in most microbial rhodopsins, the red shift of the spectrum occurs by the protonation of the primary counterion. Further acidification results in the protonation of Asp212 of BR, the secondary counterion, and the blue shifts were observed in the presence or absence of Cl^-.[45,46] In the absence of Cl^-, λ_{max} does not return to the original value at neutral pH.[45] On the other hand, in the presence of Cl^-, λ_{max} returns completely to the original and so-called acid-purple forms.[46] The similar blue shift in the presence of Cl^- was also reported in NpSRII (phoborhodopsin).[47] If a similar blue shift also occurs in PR, this method can be used in the determination of the pK_a of the secondary counterion, Asp227, of PR, which may be compared with the estimated pK_a obtained from the ITO experiments.

Figure 8 shows the pH titration of the absorbance spectra of wild-type PR at varying Cl^- concentrations, and Figure 9 shows the spectra of various mutants in the presence and absence of 4 M Cl^-. These figures indicate the existence of two phases of above and below pH 5 except for a D97N/D227N double mutant. The λ_{max} values of this mutant are constant independent of pH, indicating that above pH 5, the protonation state of Asp97 plays an important role (because the pK_a of this residue is ~7) while that of Asp227 changes the λ_{max} below pH 5. From these figures, the characteristics of λ_{max} are as follows. (1) The neutralization of the primary counterion (Asp97) results in the red shift that is the same as those of BR and other microbial rhodopsins. (2) The neutralization of the secondary counterion (Asp227) results in a blue shift, but λ_{max} seems not to return completely to that of the original pigment, which is the same as that of BR.[45,46] (3) Cl^- may bind when both Asp97 and Asp227 are neutralized, and λ_{max} of this form is longer than that in the absence of Cl^-. Finding 3 is in sharp contrast with those for BR and NpSRII. This rule holds only partially for the

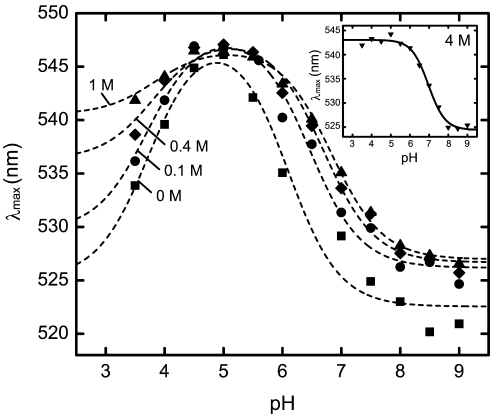

Figure 8. pH titration of the absorbance spectra of PR at varying Cl^- concentrations. The respective λ_{max} values in the presence of 0 (■), 0.1 (●), 0.4 (◆), and 1 M NaCl (▲) were plotted vs pH. The λ_{max} in the presence of 4 M NaCl (▼) is shown in the inset. The appropriate concentration of Na_2SO_4 was added to each medium to keep the total ionic strength constant. The medium contained 10 mM buffer (citrate/MES/MOPS/HEPES/CAPS/CHES), and the pH was adjusted via the addition of H_2SO_4 or NaOH.

λ_{max} shifts of D227N. Thus, we assumed the presence of the Y residue (see the Supporting Information).

From the regression analysis of these data, the pK_a values of the two counterions (pK_{a1}, the pK_a of Asp97; pK_{a2}, the pK_a of Asp227) in the dark were estimated. The details of the analysis are described in the Supporting Information. The estimated parameters (pK_{a1}, pK_{a2}, λ_{max1}, λ_{max2}, and λ_{max3}) are summarized in Table 2. Both pK_{a1} and pK_{a2} exhibited a Cl^- dependence. pK_{a1} increased with an increase in Cl^- concentration, whereas pK_{a2} decreased with an increase in Cl^- concentration. It has been reported that the pK_a of Asp97 in the dark is affected by the existence of various anions.[48] On the other hand, this paper is the first report on the dependence of the pK_a of Asp227 on Cl^- concentration. The pK_a of Asp85 of BR decreases with an increase in salt concentration,[2] whereas that of PR (Asp97) exhibits the opposite behavior. It is worth describing that, as shown in Table 2, the values of pK_{ab}, which were determined from the first proton release, are almost equal to the values of pK_{a2}, the values of Asp227 that were determined spectroscopically.

First Proton Release in Other Microbial Rhodopsins at Low pH. Here, we observed in PR the first photoinduced proton release in acidic media where the primary and secondary counterions are protonated. We investigated whether the proton release at low pH occurs in other microbial rhodopsins. We observed the first proton release in BR, XR (xanthorhodopsin), HsSRII, NpSRII, and HmSRIII (sensory rhodopsin III from *H. marismortui*), but not in ASR (*Anabaena* sensory rhodopsin) or NpHR (data not shown). The pH values at which the release was observed depended on the rhodopsins perhaps because of the different pK_a values of the second counterions of microbial rhodopsins. The residue of ASR corresponding to Asp227 of PR or Asp212 of BR is proline, and we could not observe proton release. For NpHR, the corresponding residue is also Asp252, but the release was not observed (a possible reason is described in the Discussion).

■ DISCUSSION

Important Role of Asp227 in the Early Photoinduced Proton Release. We observed the photoinduced proton

dx.doi.org/10.1021/bi300940p | *Biochemistry* 2012, 51, 9290−9301

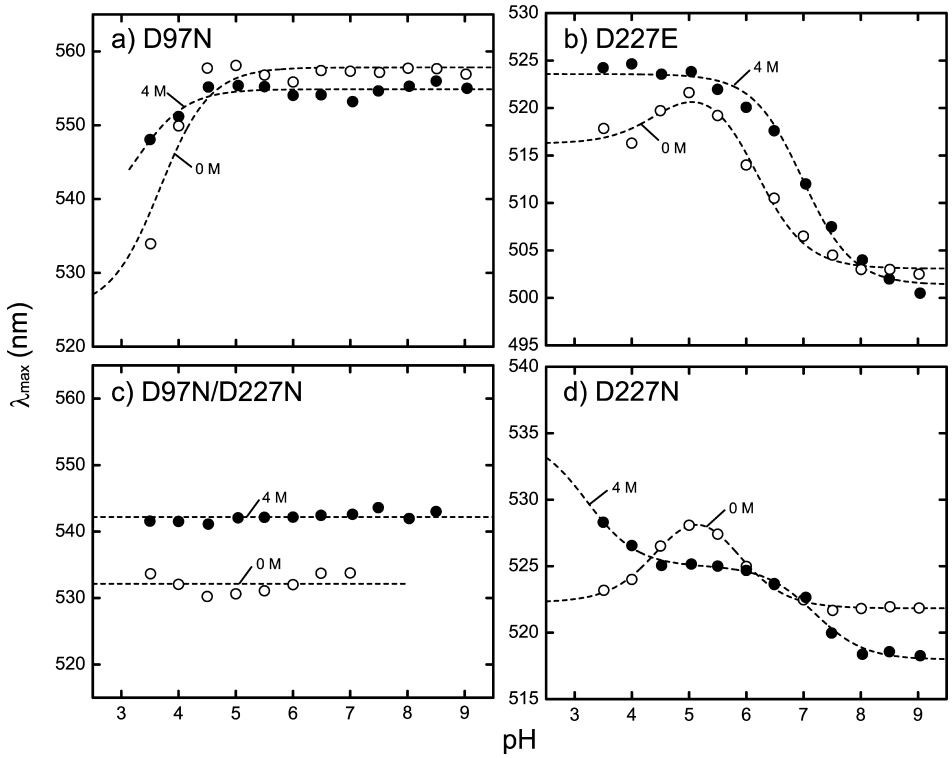

Figure 9. pH titration of the absorbance spectra of several PR mutants: (a) D97N, (b) D227E, (c) D97N/D227N, and (d) D227N. The empty and filled circles represent the λ_{max} values in the absence and presence of 4 M NaCl, respectively. The measurements were preformed in the pH range of 3.5−9. The λ_{max} value of D97N/D227N in the absence of Cl^-, on the other hand, could not be determined above pH ∼7 because of the deprotonation of the PSB in the dark.

Table 2. Parameters from the Analysis of the Absorbance Spectra[a]

	[Cl^-] (M)	pK_{a1}	pK_{a2} (pK_{ab})	λ_{max1}	λ_{max2}	λ_{max3}
WT	0	6.1	3.7 (3.5)	523	548	525
	0.1	6.5	3.6 (3.4)	526	548	525
	0.4	6.7	3.5 (3.3)	527	548	525
	1	6.8	3.3 (3.2)	527	547	525
	4	7.0	–	524	543	–
D97N	0	–	3.7	–	558	525
	0.4		(3.5)			
	4	–	3.0	–	555	520
D227E	0	6.2	4.5	503	523	516
	0.4		(4.2)			
	4	7.0	–	501	524	–

[a]The meanings of pK_{a1}, pK_{a2}, λ_{max1}, λ_{max2}, and λ_{max3} are discussed in the Supporting Information. Here, this table shows that the values of pK_{a2} (pK_a of Asp227 in the dark obtained by spectroscopy) and pK_{ab} [pK_a of Asp227 in the dark obtained from the ITO experiments (see Table 1)] are almost equal.

release and subsequent uptake (Figures 1 and 2) in PR, and the mutant experiments led to the conclusion that Asp227 and Asp97 in one case (Cl^--free D227N) are key residues controlling proton release. From Figure 2b, we estimated pK_a values for the unphotolyzed state and the proton-releasing photoproduct. The pK_a of Asp227 was also estimated spectroscopically (Supporting Information), and the estimated values were nearly equal to those obtained from the ITO experiments (Tables 1 and 2). These findings may imply that the most plausible candidate for the proton source is protonated Asp227, although we cannot rule out the possibility that the protonated water molecule inside the membrane is the source. However, even if the protonated water is a direct source, the important role of Asp227 is clear because D227N does not show the first proton release. Further studies using FTIR or D_2O are needed for clarification of the direct proton source.

Difference in the pK_a Value of the Primary and Secondary Counterions between BR and PR. As described above, although there is a possibility that the determined pK_a values in Figure 2 are not those of Asp227, we, in further discussion, assume these values (∼3.0 for the unphtolyzed state and ∼2.3 for the photolyzed state) are those of Asp227 because the value of the unphotolyzed state is nearly equal to that determined by spectroscopy (Table 2). A similar value (∼2.6) for the unphotolyzed state was obtained from the pH-dependent formation of the 430 nm species, which increases via neutralization of Asp227.[32] In BR, the pK_a of Asp212, which corresponds to Asp227 of PR, in the unphotolyzed state is considered to be very low (less than ∼1)[49] and is not yet known for the photoproducts. However, if we assume that the photoexcitation may also decrease the pK_a of Asp212 of BR, the pK_a of this BR residue in the photoproduct may be less than 0, although its determination will be difficult. The pK_a of Asp212 of BR is very low because the deprotonated state of Asp212 is stabilized by hydrogen bonds with Tyr57 and Tyr185.[50] The corresponding PR residues are also tyrosines (Tyr76 and Tyr200), but it is possible that the hydrogen bondings with these tyrosines may be weaker than the bonding obtained in those of BR. Other possible reasons for this difference in pK_a values are (i) the weak coupling of Arg94 with the chromophore and its counterion[29] and (ii) the existence of His75, which interacts with Asp97, the primary counterion, to

dx.doi.org/10.1021/bi300940p | Biochemistry 2012, 51, 9290−9301

increase its pK_a to ~7.[51] Further study is therefore necessary to ascertain the cause behind Asp227 of PR being larger than Asp212 of BR.

Possible Significance of the Transient Decrease in the pK_a of Asp227, the Secondary Counterion. In the following discussion, we assume that the photoinduced transient decrease in the pK_a of Asp227 also occurs even under neural-pH conditions, although Asp227 is deprotonated. Figure 7 indicates that the decrease in the pK_a (proton release) may occur during the decay of the L intermediate (or the decay of the K intermediate), and we assume that this change in pK_a at neutral pH occurs at the similar transition process irrespective of the presence or absence of M. The mechanism for the decrease in the pK_a of Asp227 is not yet known. However, it is possible that it can be ascribed to the changes in the hydrogen bonding network of Asp227, which include hydrogen bonding through the tyrosines and/or water.[30]

During the formation of M, the pK_a of the PSB may decrease to <4 because at pH >4, M can be observed, and the pK_a of Asp97 may increase. Therefore, the proton on the PSB is transferred to the deprotonated Asp97, the primary proton counterion. However, there is a small possibility that the proton on the PSB might be transferred to the deprotonated Asp227 because its pK_a in the dark state is ~3.0, which is not very different from the possible pK_a of the PSB during the formation of M. A small probability exists that the proton from the PSB is accepted by Asp227 to form the deprotonated Schiff base-like M intermediate. Then the pK_a of Asp227 decreased, which causes the transfer of the proton from Asp227 to Asp97. Therefore, almost all of the protons on the PSB are transferred to Asp97, but some proton may be transferred through Asp227. In other words, the low pK_a of the secondary counterion in the dark state and its photoinduced pK_a decrease hinder the transfer of the proton from the PSB to the secondary counterion.

Previously, we showed that the pH dependence of the formation of M and the proton uptake were roughly in accord with the Henderson−Hasselbalch equation using the pK_a of Asp97 in the dark,[37] but close inspection showed a small but indubitable discrepancy: in the pH region of 4−5.5, in which Asp97 is almost completely protonated (its pK_a is 6.9 or 6.8), the formation of M and proton uptake were observed (J. Tamogami et al., unpublished observations). There is a possibility that Asp227 (pK_a ~ 3) works as a proton acceptor in this pH region, assuming that the decay is very fast or the extinction coefficient of this M-like intermediate might be small. After the proton is accepted by Asp227, the pK_a of this residue decreases, thereby releasing the proton, although the timing may be different from that shown in Figure 7. The residue that accepts the proton released from Asp227 is not yet known. Further study is therefore necessary; it is possible that this might be in connection with the observation made by Bamberg and his co-workers that, under acidic conditions, PR works as an inverse proton pump.[25,52]

The pK_a value of Asp212 of BR seems much smaller (<1 in the dark and possibly ~0 in the photolyzed state) than that of PSB. Therefore, the path described above might not be probable in this microbial rhodopsin. Nevertheless, the computational calculations performed by Bondar et al. showed that there are three pathways that can occur during the primary transfer of a proton from the PSB to Asp85 of BR: (i) the direct transfer of the proton to Asp85 on the Thr89 side of the retinal, (ii) a proton wire through Thr89, and (iii) the Schiff base proton that is transferred via Asp212. The energy barrier of the third process is the smallest (11.5 kcal/mol).[53] Therefore, the pathway via Asp212 is probable even for BR, in which the pK_a of the secondary counterion is much smaller than that of the PSB.

Importance of Negative Charge at the Position of the Counterion. An unexpected and intriguing observation is shown in Figure 5, which shows the proton release in the absence of Cl^-, although the possible proton source residue (Asp227) is mutated to a proton-release-disabled residue. Figure 5b shows the disappearance of the first proton release in the case of the D97N/D227N double mutant in the absence of Cl^-. These facts reveal that for the proton release of D227N in the absence of Cl^-, Asp97 is a key residue, the primary counterion, thereby implying that the pK_a of this residue also exhibits a photoinduced decrease. Note that the pK_a of Asp97 ordinarily increases instead. Proton release, possibly the pK_a decrease, was not observed in the presence of Cl^- (panel Figure 5a,c). Therefore, it is assumed that Cl^- may bind in the vicinity of neutralized position 227 and the positively charged Arg94. These facts may imply that illumination, most likely the isomerization of retinal, requires the negative charge in the "pentagon structure" to stabilize the photoproducts. The twisted chromophore might lead to the localization of the positive charge on the π-electron chain of the protonated chromophore, or to a hydrophobic circumstance because of the movement of the water molecule, which causes the increase in the strength of an electrical interaction to need the negative charge. Then, under physiological conditions, the negatively charged secondary counterion may serve this purpose. If no negative charge exists nearby, the negative charge is most likely produced through the deprotonation of the secondary counterion; if this does not occur, binding with Cl^- probably takes place. If these two mechanisms cannot occur, the primary counterion is forced to be deprotonated to an anionic form, although the possibility that a proton is released from a protonated water is not ruled out. Thus, we can hypothesize that this negative charge at the secondary counterion position hinders the decrease in pK_a in the primary counterion. Moreover, we may assume that this negative charge contributes to the increase in the pK_a of the primary counterion.

The D212N BR mutant does not exhibit proton pumping activity in the absence of Cl^-; this activity is restored with Cl^- binding.[54] Therefore, the same molecular mechanism that was found in the PR D227N mutant may occur in this BR mutant. If the negative charge at the secondary counterion position does not exist, the decrease in pK_a in the primary counterion may happen, which hinders the proper transfer of the proton from the PSB to the primary counterion. Consequently, M is not formed. In addition, Shibata et al. proposed a model in which the binding of Cl^- around Arg82 of BR induces the proper arrangement of the hydrogen bonding network around the Schiff base and restores the H^+ pumping activity of this mutant.[55]

We also observed a similar proton release at low pH in other microbial rhodopsins, with the exception of ASR and NpHR. For ASR, the lack of the corresponding Asp residue may be the reason for the lack of release. If negative charge is necessary for isomerization, how is the negative charge in ASR produced? For NpHR, if Cl^- is bound even under acidic conditions, the proton release may not occur because of its negative charge.

dx.doi.org/10.1021/bi300940p | *Biochemistry* 2012, 51, 9290−9301

CONCLUSIONS

In this study, we found that illumination induces the early release of a proton from PR below pH ~4, where the primary (Asp97) and secondary (Asp227) counterions are protonated. From the pH dependence of the amounts of proton released, we estimated the pK_a values of the photolyzed (~2.3) and unphotolyzed (~3.0) states. Mutation experiments showed that Asp227 is a key residue. The pK_a of Asp227 was determined spectroscopically, and the values obtained were approximately equal to that estimated as an unphotolyzed value in the ITO experiment. Then, it is probable that the proton source is Asp227, although we cannot rule out the possibility that the source is protonated water. Further study is needed to clarify what is a direct source using FTIR. From results obtained using mutants of Asp97 and/or Asp227 with and without Cl^-, we concluded that the presence of the negative charge near the Schiff base is indispensable for the stabilization of the photoproducts, and thus, the negative charge of Asp227 under physiological conditions plays an import role in the isomerization from K or L to M. Another possible significance of the decrease in the pK_a of the secondary counterion of PR is that it is supposed to conduct the transfer of the proton from the Schiff base to the primary counterion, not to the symmetrically located secondary counterion.

ASSOCIATED CONTENT

Supporting Information

Reason and validity of the use of 1 mM buffer solutions (Figures S1 and S2), absorbance spectra of wild-type PR and its mutants at various pH values in the absence of Cl^- (Figure S3), absorbance spectra of wild-type PR in the presence of Cl^- (Figure S4), and detailed descriptions of the method of the analysis of the pH-dependent absorbance spectral changes of wild-type PR and its mutants. This material is available free of charge via the Internet at http://pubs.acs.org.

AUTHOR INFORMATION

Corresponding Author

*Telephone: +81-(0)89-925-7111. Fax: +81-(0)89-926-7138. E-mail: jtamoga@cc.matsuyama-u.ac.jp.

Funding

This work was supported by grants from the Japanese Ministry of Education, Culture, Sports, Science, and Technology to J.T. (23790059) and N.K. (22590049).

Notes

The authors declare no competing financial interest.

ACKNOWLEDGMENTS

We thank Dr. Oded Béjà and Dr. Kwang-Hwan Jung for providing the expression plasmids of PR and ASR, respectively. We also thank Dr. Janos K. Lanyi and Dr. Sergei P. Balashov for providing the XR proteins.

ABBREVIATIONS

PR, proteorhodopsin; BR, bacteriorhodopsin; HR, halorhodopsin; SRI, sensory rhodopsin I; SRII, sensory rhodopsin II; HsSRII, SRII from *H. salinarum*; NpSRII, SRII from *N. pharaonis*; ASR, *Anabaena* sensory rhodopsin; XR, xanthorhodopsin; HmSRIII, sensory rhodopsin III from *H. marismortui*; SB, deprotonated Schiff base; PSB, protonated Schiff base; λ_{max}, maximal absorption wavelength; ITO, indium−tin oxide; PC, L-α-phosphatidylcholine; MES, HEPES, MOPS, CAPS, and CHES, known abbreviations of Good's buffers.

REFERENCES

(1) Haupts, U., Tittor, J., and Oesterhelt, D. (1999) Closing in on bacterorhodopsin: Progress in understanding the molecule. *Annu. Rev. Biophys. Biomol. Struct. 28*, 367−399.

(2) Balashov, S. P. (2000) Protonation reactions and their coupling in bacteriorhodopsin. *Biochim. Biophys. Acta 1460*, 75−94.

(3) Mukohata, Y., Ihara, K., Tamura, T., and Sugiyama, Y. (1999) Halobacterial rhodopsins. *J. Biochem. 125*, 649−657.

(4) Váró, G. (2000) Analogies between halorhodopsin and bacteriorhodopsin. *Biochim. Biophys. Acta 1460*, 220−229.

(5) Essen, L. O. (2002) Halorhodopsin: Light-driven ion pumping made simple? *Curr. Opin. Struct. Biol. 12*, 516−522.

(6) Bogomolni, R. A., and Spudich, J. L. (1982) Identification of a third rhodopsin-like pigment in phototactic *Halobacterium halobium*. *Proc. Natl. Acad. Sci. U.S.A. 79*, 6250−6254.

(7) Hazemoto, N., Kamo, N., Terayama, Y., Kobatake, Y., and Tsuda, M. (1983) Photochemistry of 2 rhodopsinlike pigments in bacteriorhodopsin-free mutant of *Halobacterium halobium*. *Biophys. J. 44*, 59−64.

(8) Spudich, J. L., and Bogomolni, R. A. (1984) Mechanism of color discrimination by a bacterial sensory rhodopsin. *Nature 312*, 509−513.

(9) Takahashi, T., Tomioka, H., Kamo, N., and Kobatake, Y. (1985) A photosystem other than P370 also mediates the negative phototaxis of *Halobacterium halobium*. *FEMS Microbiol. Lett. 28*, 161−164.

(10) Wolff, E. K., Bogomolni, R. A., Scherrer, P., Hess, B., and Stoeckenius, W. (1986) Color discrimination in halobacteria: Spectroscopic characterization of a second sensory receptor covering the blue-green region of the spectrum. *Proc. Natl. Acad. Sci. U.S.A. 83*, 7272−7276.

(11) Spudich, E. N., Sundberg, S. A., Manor, D., and Spudich, J. L. (1986) Properties of a second sensory receptor protein in *Halobacterium halobium* phototaxis. *Proteins 1*, 239−246.

(12) Marwan, W., and Oesterhelt, D. (1987) Signal formation in the halobacterial photophobic response mediated by a fourth retinal protein (P480). *J. Mol. Biol. 195*, 333−342.

(13) Béjà, O., Aravind, L., Koonin, E. V., Suzuki, M. T., Hadd, A., Nguyen, L. P., Jovanovich, S. B., Gates, C. M., Feldman, R. A., Spudich, J. L., Spudich, E. N., and DeLong, E. F. (2000) Bacterial rhodopsin: Evidence for a new type of phototrophy in the sea. *Science 289*, 1902−1906.

(14) Jung, K.-H., Trivedi, V. D., and Spudich, J. L. (2003) Demonstration of a sensory rhodopsin in eubacteria. *Mol. Microbiol. 47*, 1513−1522.

(15) Balashov, S. P., Imasheva, E. S., Boichenko, V. A., Antón, J., Wang, J. M., and Lanyi, J. K. (2005) Xanthorhodopsin: A proton pump with a light-harvesting carotenoid antenna. *Science 309*, 2061−2064.

(16) Bieszke, J. A., Spudich, E. N., Scott, K. L., Borkovich, K. A., and Spudich, J. L. (1999) A eukaryotic protein, NOP-1, binds retinal to form an archaeal rhodopsin-like photochemically reactive pigment. *Biochemistry 38*, 14138−14145.

(17) Waschuk, S. A., Bezerra, A. G., Shi, L., Jr., and Brown, L. S. (2005) *Leptosphaeria* rhodopsin: Bacteriorhodopsin-like proton pump from a eukaryote. *Proc. Natl. Acad. Sci. U.S.A. 102*, 6879−6883.

(18) Kateriya, S., Nagel, G., Bamberg, E., and Hegemann, P. (2004) "Vision" in Single-Celled Algae. *News Physiol. Sci. 19*, 133−137.

(19) Tsunoda, S. P., Ewers, D., Gazzarrini, S., Moroni, A., Gradmann, D., and Hegeman, P. (2006) H^+-pumping rhodopsin from the marine alga *Acetabularia*. *Biophys. J. 91*, 1471−1479.

(20) Wada, T., Shimono, K., Kikukawa, T., Hato, M., Shinya, N., Kim, S.-Y., Kimura-Someya, T., Shirouzu, M., Tamogami, J., Miyauchi, S., Jung, K.-H., Kamo, N., and Yokoyama, S. (2011) Crystal structure of the eukaryotic light-driven proton pumping rhodopsin, *Acetabularia* rhodopsin II, from marine alga. *J. Mol. Biol. 411*, 986−998.

(21) Kikukawa, T., Shimono, K., Tamogami, J., Miyauchi, S., Kim, S.-Y., Kimura-Someya, T., Shirouzu, M., Jung, K.-H., Yokoyama, S., and

Kamo, N. (2011) Photochemistry of *Acetabularia* rhodopsin II from a marine plant, *Acetabularia acetabulum*. *Biochemistry 50*, 8888−8898.
(22) Fuhrman, J. A., Schwalbach, M. S., and Stingl, U. (2009) Proteorhodopsins: An array of physiological roles? *Nat. Rev. Microbiol. 6*, 488−494.
(23) Venter, J. C., Remington, K., Heidelberg, J. F., Halpern, A. L., Rusch, D., Eisen, J. A., Wu, D., Paulsen, I., Nelson, K. E., Nelson, W., Fouts, D. E., Levy, S., Knap, A. H., Lomas, M. W., Nealson, K., White, O., Peterson, J., Hoffman, J., Parsons, R., Baden-Tillson, H., Pfannkoch, C., Rogers, Y.-H., and Smith, H. O. (2004) Environmental genome shotgun sequencing of the Sargasso Sea. *Science 304*, 58−60.
(24) Dioumaev, A. K., Brown, L. S., Shih, J., Spudich, E. N., Spudich, J. L., and Lanyi, J. K. (2002) Proton transfers in the photochemical reaction cycle of proteorhodopsin. *Biochemistry 41*, 5348−5358.
(25) Friedrich, T., Geibel, S., Kalmbach, R., Chizhov, I., Ataka, K., Heberle, J., Engelhard, M., and Bamberg, E. (2002) Proteorhodopsin is a light-driven proton pump with variable vectoriality. *J. Mol. Biol. 321*, 821−838.
(26) Váró, G., Brown, L. S., Lakatos, M., and Lanyi, J. K. (2003) Characterization of the photochemical reaction cycle of proteorhodopsin. *Biophys. J. 84*, 1202−1207.
(27) Lakatos, M., Lanyi, J. K., Szakács, J., and Váró, G. (2003) The photochemical reaction cycle of proteorhodopsin at low pH. *Biophys. J. 84*, 3252−3256.
(28) Dioumaev, A. K., Wang, J. M., Bálint, Z., Váró, G., and Lanyi, J. K. (2003) Proton transport by proteorhodopsin requires that the retinal Schiff base counterion Asp-97 be anionic. *Biochemistry 42*, 6582−6587.
(29) Partha, R., Krebs, R., Caterino, T. L., and Braiman, M. S. (2005) Weakened coupling of conserved arginine to the proteorhodopsin chromophore and its counterion implies structural differences from bacteriorhodopsin. *Biochim. Biophys. Acta 1708*, 6−12.
(30) Ikeda, D., Furutani, Y., and Kandori, H. (2007) FTIR study of the retinal Schiff base and internal water molecules of proteorhodopsin. *Biochemistry 46*, 5365−5373.
(31) Rupenyan, A., van Stokkum, I. H. M., Arents, J. C., van Grondelle, R., Hellingwerf, K., and Groot, M. L. (2008) Characterization of the primary photochemistry of proteorhodopsin with femtosecond spectroscopy. *Biophys. J. 94*, 4020−4030.
(32) Imasheva, E. S., Balashov, S. P., Wang, J. M., Dioumaev, A. K., and Lanyi, J. K. (2004) Selectivity of retinal photoisomerization in proteorhodopsin is controlled by aspartic acid 227. *Biochemistry 43*, 1648−1655.
(33) Imasheva, E. S., Shimono, K., Balashov, S. P., Wang, J. M., Zadok, U., Sheves, M., Kamo, N., and Lanyi, J. K. (2005) Formation of a long-lived photoproduct with a deprotonated Schiff base in proteorhodopsin, and its enhancement by mutation of Asp227. *Biochemistry 44*, 10828−10838.
(34) Heberle, J. (2000) Proton transfer reactions across bacteriorhodopsin and along the membrane. *Biochim. Biophys. Acta 1458*, 135−147.
(35) Miyasaka, T., Koyama, K., and Itoh, I. (1992) Quantum conversion and image detection by a bacteriorhodopsin-based artificial photoreceptor. *Science 255*, 342−344.
(36) Koyama, K., Miyasaka, T., Needleman, R., and Lanyi, J. K. (1998) Photoelectrochemical verification of proton-releasing groups in bacteriorhodopsin. *Photochem. Photobiol. 68*, 400−406.
(37) Tamogami, J., Kikukawa, T., Miyauchi, S., Muneyuki, E., and Kamo, N. (2009) A tin oxide transparent electrode provides the means for rapid time-resolved pH measurements: Application to photoinduced proton transfer of bacteriorhodopsin and proteorhodopsin. *Photochem. Photobiol. 85*, 578−589.
(38) Tamogami, J., Kikukawa, T., Ikeda, Y., Takemura, A., Demura, M., and Kamo, N. (2010) The photochemical reaction cycle and photoinduced proton transfer of sensory rhodopsin II (phoborhodopsin) from *Halobacterium salinarum*. *Biophys. J. 98*, 1353−1363.
(39) Kandori, H., Shimono, K., Sudo, Y., Iwamoto, M., Shichida, Y., and Kamo, N. (2001) Structural changes of *pharaonis* phoborhodopsin upon photoisomerization of the retinal chromophore: Infrared spectral comparison with bacteriorhodopsin. *Biochemistry 40*, 9238−9246.
(40) Nakao, Y., Kikukawa, T., Shimono, K., Tamogami, J., Kimitsuki, N., Nara, T., Unno, M., Ihara, K., and Kamo, N. (2011) Photochemistry of a putative new class of sensory rhodopsin (SRIII) coded by *xop2* of *Haloarcular marismortui*. *J. Photochem. Photobiol., B 102*, 45−54.
(41) Becher, B., and Cassim, J. T. (1975) Improved isolation procedures for the purple membrane of *Halobacterium halobium*. *Prep. Biochem. 5*, 161−178.
(42) Chizhov, I., Schmies, G., Seidel, R., Sydor, J. R., Lüttenberg, B., and Engelhard, M. (1998) The photophobic receptor from *Natronobacterium pharaonis*: Temperature and pH dependencies of the photocycle of sensory rhodopsin II. *Biophys. J. 75*, 999−1009.
(43) Sato, M., Kikukawa, T., Araiso, T., Okita, H., Shimono, K., Kamo, N., Demura, M., and Nitta, K. (2003) Role of Ser130 and Thr126 in chloride binding and photocycle of *pharaonis* halorhodopsin. *J. Biochem. 134*, 151−158.
(44) Tateishi, Y., Abe, T., Tamogami, J., Nakao, Y., Kikukawa, T., Kamo, N., and Unno, M. (2011) Spectroscopic evidence for the formation of an N intermediate during the photocycle of sensory rhodopsin II (phoborhodopsin) from *Natronobacterium pharaonis*. *Biochemistry 50*, 2135−2143.
(45) Balashov, S. P., Govindjee, R., Imasheva, E., Misra, M., Ebrey, T. G., Feng, Y., Crouch, R. K., and Menick, D. R. (1995) The two pK_a's of aspartate-85 and control of thermal isomerization and proton release in the arginine-82 to lysine mutant of bacteriorhodopsin. *Biochemistry 34*, 8820−8834.
(46) Kelemen, L., Galajda, P., Száraz, S., and Ormos, P. (1999) Chloride ion binding to bacteriorhodopsin at low pH: An infrared spectroscopic study. *Biophys. J. 76*, 1951−1958.
(47) Shimono, K., Kitami, M., Iwamoto, M., and Kamo, N. (2000) Involvement of two groups in reversal of the bathochromic shift of *pharaonis* phoborhodopsin by chloride at low pH. *Biophys. Chem. 87*, 225−230.
(48) Sharaabi, Y., Brumfeld, V., and Sheves, M. (2010) Binding of anions to proteorhodopsin affects the Asp97 pK_a. *Biochemistry 49*, 4457−4465.
(49) Metz, G., Siebert, F., and Engelhard, M. (1992) Asp^{85} is the only internal aspartic acid that gets protonated in the M intermediate and the purple-to-blue transition of bacteriorhodopsin. A solid-state ^{13}C CP-MAS NMR investigation. *FEBS Lett. 303*, 237−241.
(50) Lanyi, J. K. (2006) Proton transfers in the bacteriorhodopsin photocycle. *Biochim. Biophys. Acta 1757*, 1012−1018.
(51) Bergo, V. B., Sineshchekov, O. A., Kralj, J. M., Partha, R., Spudich, E. N., Rothschild, K. J., and Spudich, J. L. (2009) His-75 in proteorhodopsin, a novel component in light-driven proton translocation by primary pumps. *J. Biol. Chem. 284*, 2836−2843.
(52) Lörinczi, É., Verhoefen, M.-K., Wachtveitl, J., Woerner, A. C., Glaubitz, C., Engelhard, M., Bamberg, E., and Friedrich, T. (2009) Voltage- and pH-dependent changes in vectoriality of photocurrents mediated by wild-type and mutant proteorhodopsins upon expression in *Xenopus* oocytes. *J. Mol. Biol. 393*, 320−341.
(53) Bondar, A.-N., Elstner, M., Suhai, S., Smith, J. C., and Fischer, S. (2004) Mechanism of primary proton transfer in bacteriorhodopsin. *Structure 12*, 1281−1288.
(54) Moltke, S., Krebs, M. P., Mollaaghababa, R., Khorana, H. G., and Heyn, M. P. (1995) Intramolecular charge transfer in the bacteriorhodopsin mutants Asp85→Asn and Asp2l2→Asn: Effects of pH and anions. *Biophys. J. 69*, 2074−2083.
(55) Shibata, M., Yoshitsugu, M., Mizuide, N., Ihara, K., and Kandori, H. (2007) Halide binding by the D212N mutant of bacteriorhodopsin affects hydrogen bonding of water in the active site. *Biochemistry 46*, 7525−7535.